DOI: https://doi.org/10.54966/jreen.v1i1.1269

Journal of Renewable Energies

Revue des Energies Renouvelables

journal home page: https://revue.cder.dz/index.php/rer

Conference paper

Predictive current control implementation of Stand Alone PV inverter

Mohamed Rida Bengourina [a,*], **Linda Hassaine** [a], **Fateh Abdoune** [a], **Issam Abadlia** [a]

[a] *Centre de Developpement des Energies Renouvelables, CDER, BP 62 Route de l'Observatoire, Bouzaréah, 16340, Algiers, Algeria*

ARTICLE INFO

Article history:

Received August 1st, 2024
Accepted Sptember 4, 2024

Keywords:

Photovoltaic,
Inverter,
MPCC,
Load,
Resistor,
Inductor.

ABSTRACT

In stand-alone photovoltaic (PV) systems, the main goal is to control the current that the inverter feeds to the load. In this paper, the performance of predictive current control (MPCC) is tested and evaluated for a stand-alone photovoltaic (PV) system. Our evaluation spans various current amplitudes and frequencies, aiming to demonstrate its robust performance and practical applicability. The MPCC method employs a discrete-time model of the system, enabling the prediction of future values of the load current for all potential volt-age vectors generated by the inverter. Implementing the MPCC strategy on RL (resistor-inductor) load alimented by a PV inverter offers the advantage of simplified implementation and significantly reduced computing time. Simulation and experimental results are presented to prove the efficiency and practical applicability of the proposed control. Both results conclusively demonstrate the high efficacy of MPCC in managing a stand-alone photovoltaic (PV) inverter across various current amplitudes and frequencies, ensuring reliable and robust performance

1. INTRODUCTION

In the last few decades, power electronic systems and electrical drives have drawn significant revolution in a broad range of industrial applications. This is mainly due to the advancement in power semiconductor devices, converter topologies, control methods, and micro-controller resources (Bose 2000). The control of power converters has been extensively studied, and new control schemes are presented every year. Most prominently, the development of control methods is progressing well for the newly emerged sophisticated applications which may have multiple control targets, system constraints, and functionalities…etc (Kouro & al 2015).

* *Corresponding author, E-mail address: m.bengourina@cder.dz*

ISSN: 1112-2242 / EISSN: 2716-8247

Various current control strategies have been suggested for controlling power converters, but hysteresis control and linear control employing pulse-width modulation (PWM) stand out as the most widely used in the literature.(Xiaowei & al 2021; Wensheng & al 2016; Qin & al 2012; Hassaine, L., Bengourina, M.R. 2020). However, with the development of faster and more powerful microprocessors, the implementation of new and more complex control schemes become possible (Dadu, A,. Mekhilef, S. 2019; Rodriguez, J., Cortes, P. 2012; Wang & al 2015). Some of these new control schemes for power converters include fuzzy logic, sliding mode control and predictive control. The MPC was originally introduced in the process industry with success for several decades (Rodriguez, J., Cortes, P. 2012). The complex model and slow dynamics of the process industry made it compatible with the available control platform for the implementation (Wang & al 2015; Mohamed & al 2013), however, there are many advantages with this control method. Among these advantages are relatively easy to implement and understand, fast dynamic response, and can be applied to various types of voltage source converters. The rapid advancements in microprocessor technology have facilitated the integration of MPCC into VSI converters.

This work presents an MPCC scheme for a three-phase, PV inverter-fed RL-load. The modeling of PV inverter and the load will be presented, the working principle will be explained and both simulation and experimental results will be shown.

2. SYSTEM DESCRIPTION

Generally, the PV systems are commonly categorized into grid connected systems and stand alone systems. The second are indeed particularly useful in isolated site like the rural areas. In this work, a single stage stand-alone PV system without storage energy was presented. It consist of solar panels, inverter and one or more loads.

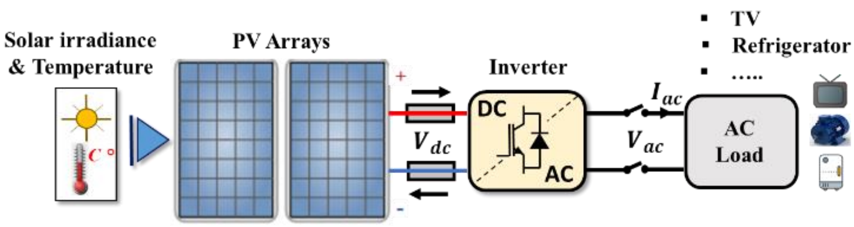

Fig 1. Stand alone PV system

2.1 Inverter model

The power circuit of the three-phase inverter converts electrical power from DC to AC form using the electrical scheme shown in Fig 2. Considering that the two switches in each inverter phase operate in a complementary mode in order to avoid short-circuiting.

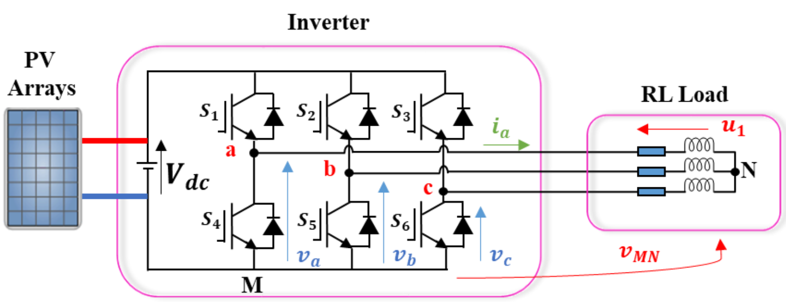

Fig 2. Voltage source inverter power circuit

The DC source, the switching state of the power switches Sx, with x = 1,…,6, can be represented by the switching signals Sa, Sb, and Sc defined as follows:

$$S_a = \begin{cases} 1 \; if \; S_1 \; on \; and \; S_4 \; off \\ 0 \; if \; S_1 \; off \; and \; S_4 \; on \end{cases} \tag{1}$$

$$S_b = \begin{cases} 1 \; if \; S_2 \; on \; and \; S_5 \; off \\ 0 \; if \; S_2 \; off \; and \; S_5 \; on \end{cases} \tag{2}$$

$$S_c = \begin{cases} 1 \; if \; S_3 \; on \; and \; S_6 \; off \\ 0 \; if \; S_3 \; off \; and \; S_6 \; on \end{cases} \tag{3}$$

By applying Kirchhoff's first law we get:

$$\begin{cases} u_1 = v_{MN} + v_a \\ u_2 = v_{MN} + v_b \\ u_3 = v_{MN} + v_c \end{cases} \tag{4}$$

With

$$v_{MN} = -\frac{1}{3}(v_a + v_b + v_c) \tag{5}$$

Replacing $\boldsymbol{v_{MN}}$ in Eq. (4) and considering that the load is balanced, we result in the following system that will be implemented in MATLAB:

$$\begin{pmatrix} u_1 \\ u_2 \\ u_3 \end{pmatrix} = \frac{1}{3} V_{dc} \begin{pmatrix} 2 & -1 & -1 \\ -1 & 2 & -1 \\ -1 & -1 & 2 \end{pmatrix} \begin{pmatrix} S_a \\ S_b \\ S_c \end{pmatrix} \tag{6}$$

Table 1. Switching states and voltage

S_a	S_b	S_c	u_1	u_2	u_3
0	0	0	0	0	0
1	0	0	2/3 V_{dc}	-1/3 V_{dc}	-1/3 V_{dc}
1	1	0	1/3 V_{dc}	1/3 V_{dc}	-2/3 V_{dc}
0	1	0	-1/3 V_{dc}	1/3 V_{dc}	-2/3 V_{dc}
0	1	1	-2/3 V_{dc}	2/3 V_{dc}	1/3 V_{dc}
0	0	1	-1/3 V_{dc}	-1/3 V_{dc}	2/3 V_{dc}
1	0	1	1/3 V_{dc}	-2/3 V_{dc}	1/3 V_{dc}
1	1	1	0	0	0

2.2 Load model

The application of Kirchhoff's first law to the RL-load in Figure 2, gives:

$$\begin{cases} u_1 = L\dfrac{di_a}{dt} + Ri_a \\ u_2 = L\dfrac{di_b}{dt} + Ri_b \\ u_3 = L\dfrac{di_c}{dt} + Ri_c \end{cases} \tag{7}$$

Where R is the load resistance and L the load inductance. By transforming Eq. (7) into Laplace domain as transfer functions, to get a model for this RL load for simulation in MATLAB/Simulink environment we get:

$$\begin{cases} \dfrac{i_a}{u_1} = \dfrac{1}{SL + R} \\ \dfrac{i_b}{u_2} = \dfrac{1}{SL + R} \\ \dfrac{i_c}{u_3} = \dfrac{1}{SL + R} \end{cases} \tag{8}$$

To achieve a precise control strategy, a forward Euler method discretization of the system Eq. (7) is utilized to accurately predict the future values of the output current at the sampling period *Ts*. So *di/dt* is replaced by *(i[k+1]-i[k])/Ts* and after some arrangements, Eq. (9) becomes:

$$\begin{cases} i_a[k+1] = \left(1 - \dfrac{RT_s}{L}\right) i_a[k] + \dfrac{u_1 T_s}{L} \\ i_b[k+1] = \left(1 - \dfrac{RT_s}{L}\right) i_b[k] + \dfrac{u_2 T_s}{L} \\ i_c[k+1] = \left(1 - \dfrac{RT_s}{L}\right) i_c[k] + \dfrac{u_3 T_s}{L} \end{cases} \tag{9}$$

Where, in the control algorithm, *ia [k]* is evaluated as the measured current of phase a at the sample k and *ia [k+1]* is evaluated as the predicted value of the current of phase a at the sample *k+1*.

3. MODEL PREDICTIVE CONTROL

MPC exploits the discrete-time model of the inverter to predict the future behavior of the current, for each switching state. Thereafter, the optimum switching state ***xopt*** is selected, based on the minimization of the cost function, and directly fed to the power switches of the converter in each sampling interval ***Ts*** (Rodriguez, J., Cortes, P. 2012; Sharida & al 2024).

3.1 Cost function

We choose the cost function to be minimize so as to achieve the lowest error between the predicted current and the reference values; which is expressed as:

$$J = |i_a[k+1] - i_a^*[k+1]| + |i_b[k+1] - i_b^*[k+1]| + |i_c[k+1] - i_c^*[k+1]| \tag{10}$$

Where $i_a^*[k+1]$, $i_b^*[k+1]$ and $i_c^*[k+1]$ are the reference values of the phase currents at the sample k+1.

3.2 Working principle

The goal of the MPCC scheme is to select an actuation that minimizes the cost function. The selected actuation is called the optimal switching state ***xopt***. The working principle is explained in the following figures:

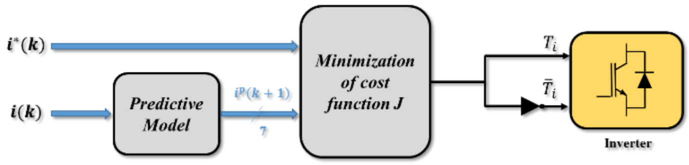

Fig 3. Predictive current control block diagram

The working principle of this control strategy is explained in detail in figure 5. The MPCC scheme uses finite number of valid switching states of the inverter in order to find the ***xopt*** by using the following steps:

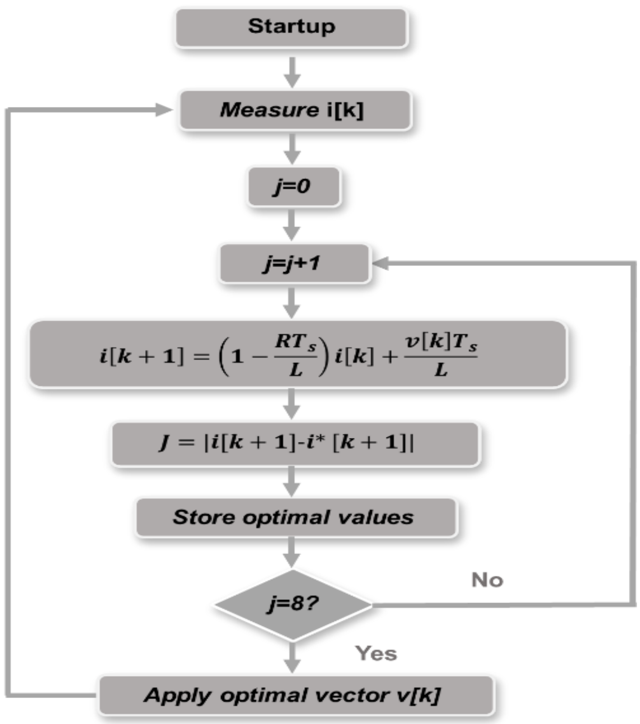

Fig 4. Flow diagram of MPCC.

1) Measure the controlled variable i[k] and estimate i*[k+1].
2) Apply the optimal switching state (computed in the previous sampling period) to calculate the output voltage of the inverter v[k] using the inverter model.
3) For every switching state of the converter, predict (using the mathematical mod-el) the behavior of current in the next sampling interval i[k+1].
4) Evaluate the cost function, or error, for each prediction as, for instance: J=|i[k+1]-i* [k+1]|.
5) Select the switching state that minimizes the cost function, S opt and store it so that it can be applied to the converter in the next sampling period.

In the implementation, we should express, the currents and the output voltage of the inverter in αβ coordinate system, to simplify and minimize the computation time as follow:

$$v = \frac{2}{3}(v_a + av_b + a^2 v_c) \quad (11)$$

$$i = \frac{2}{3}(v_a + av_b + a^2 v_c) \quad (12)$$

Where:

$a = e^{\frac{j2\pi}{3}} = -\frac{1}{2} + j\frac{\sqrt{3}}{2}$

$i_{\propto} = Re(i)\ and\ i_{\beta} = Im(i)$

Instead of calculating the output voltage of the inverter for each possible switching state at every iteration, we can calculate them in advance and apply them to the load model.

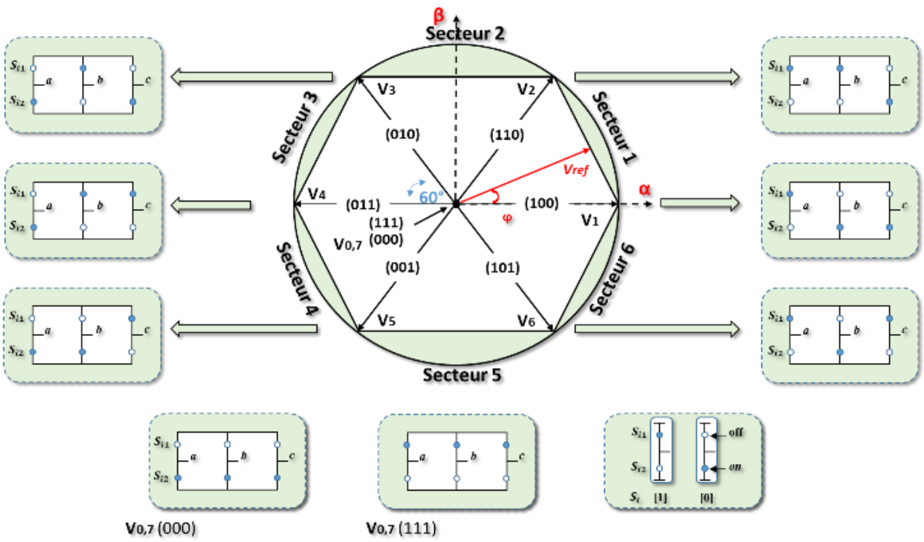

Fig 5. Eight possible combinations of the switching signals, and their corresponding voltage vectors generated by the inverter in the complex plane

Table 2. Possible switching states and output vector voltage

S_a	S_b	S_c	v
0	0	0	$v_0 = 0$
1	0	0	$v_1 = 2/3\ V_{dc}$
1	1	0	$v_2 = 1/3\ V_{dc} + j\sqrt{3}/2V_{dc}$
0	1	0	$v_3 = -1/3\ V_{dc} + j\sqrt{3}/2V_{dc}$
0	1	1	$v_4 = -2/3\ V_{dc}$
0	0	1	$v_5 = -1/3\ V_{dc} - j\sqrt{3}/2V_{dc}$
1	0	1	$v_6 = 1/3\ V_{dc} - j\sqrt{3}/2V_{dc}$
1	1	1	$v_7 = 0$

In order to reduce the number of calculations for the output current, we can transform the three equations in Eq. (9) into one equation using Eq. (12). We obtain:

$$i[k+1] = \left(1 - \frac{RT_s}{L}\right) i[k] + \frac{vT_s}{L} \tag{13}$$

Thus, the cost function becomes:

$$J = |i[k+1] - i^*[k+1]| \tag{14}$$

The output voltage vectors of the inverter are stored and selected rather than calculated each sampling period of the algorithm. The calculation of the cost function is a subtraction of two one-dimensional complex variables rather than three-dimensional variables. So, the number of calculations is considerably reduced.

4. SIMULATION AND EXPERIMENTAL RESULTS

Simulation setup was developed using Matlab/Simulink to evaluate the performance of the proposed MPCC method and experimental tests were conducted with the prototype in Fig.6. A MicroLabBox dSPACE was used to implement the proposed strategy.

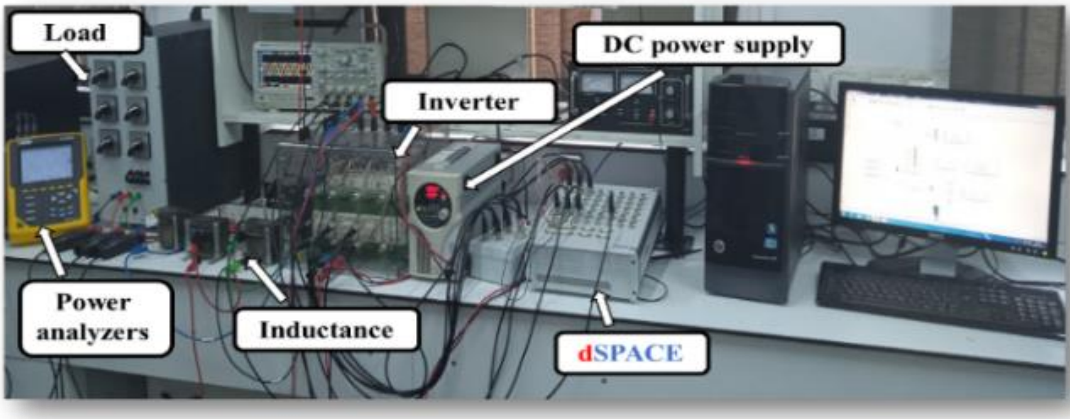

Fig 6. Experimental platform

The parameters of the simulation and experimental system are: Vdc=100V, R=10Ω, L=6mH. The output current of three phase are shown in Figure 7. During the dynamic performance evaluation, two specific test conditions are taken into account to assess the efficacy of the MPCC method the magnitude and frequency.

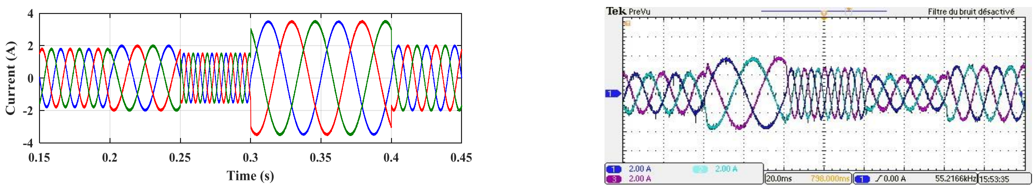

Fig 7. Simulation and experimental results of: output current of three phase.

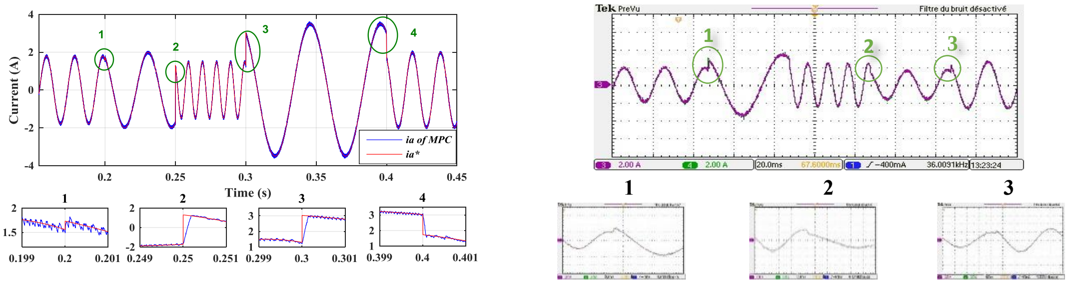

Fig 8. Simulation and experimental results of: reference and output current of phase (a) and their zoom.

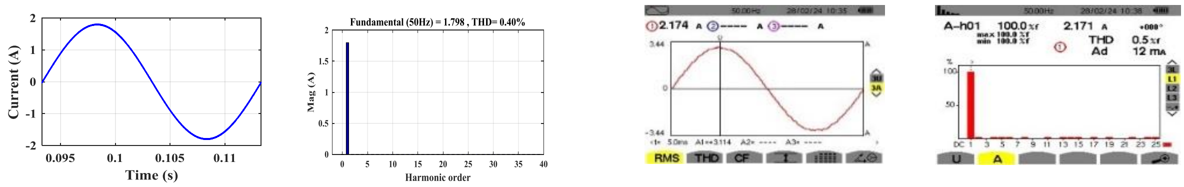

Fig 9. Simulation and experimental results of: output current of phase (a) and their THD.

Figure 8 shows that for the different references, the output current tracks the reference in short response time. Case 1: The current reference is jumped from i_a^*=1.8A with output frequency f^*=50Hz to i_a^*=2A with output frequency f^*=30Hz. Case 2: The current reference is jumped from i_a^*=2A with output frequency f^*=30Hz to i_a^*=1.5A with output frequency f^*=80Hz. Case 3: The current reference is jumped from i_a^*=1.5A with output frequency f^*=80Hz to i_a^*=3A with output frequency f^*=20Hz. Case 4: The current reference is jumped from i_a^*=3A with output frequency f^*=20Hz to i_a^*=2A with output frequency f^*=50Hz.

In all cases the inverter's reaches the current references within time lower than 0.001s. We can see that the method demonstrates excellent and nearly identical dynamic performance after any change in its magnitude and frequency. In Fig. 9, the harmonic spectrum of phase (a) current is depicted. With the MPCC method, the total harmonic distortion (THD) of inverter phase (a) current in simulation is 0.40%. While in experimental conditions, the corresponding THD of phase (a) current is 0.5%.These results show that the method can track the current references successfully with sinusoidal output currents.

5. CONCLUSION

A predictive current control strategy has been presented and implemented. It has been demonstrated that the method is highly effective in regulating load currents with a robust dynamic response. The control scheme has been simulated in Matlab/Simulink environment and tested on an experimental platform for various sampling frequencies and different reference values. Results, show that the load cur-rent successfully track its reference signal and its quality gets better with high sampling frequencies (low THD). Results of simulations and experimentals discussed in this work demonstrate the efficient and robustness of proposed strategy.

REFERENCES

Bose, B.K. (2000) Energy, environment, and advances in power electronics. IEEE Trans on Power Electronics, 15(4), 688–701. doi: https://doi.org/ 10.1109/63.849039.

Dadu, A,. Mekhilef, S. (2019) Lyapunov model predictive control to optimize computational bur-den, reference tracking and THD of three-phase four-leg inverter. IET Power Electronics, 12(05), 1061–1070. https://doi.org/10.1049/iet-pel.2018.5732.

Hassaine, L., Bengourina, M.R. (2020) Design and control technique for single phase bipolar H-bridge inverter connected to the grid. International Journal of Electrical and Computer Engineering, 10(03), 3057–3065. http://doi.org/10.11591/ijece.v10i3.pp3057-3065.

Kouro, S., Perez, M.A, Rodriguez, J., Llor, M.A., Young, H. A. (2015) Model predictive control: MPC's role in the evolution of power electronics. IEEE Ind. Electron. Mag, 9(4), 8–21. doi: https://doi.org/ 10.1109/MIE.2015.2478920.

Mohamed, I.S., Zaid, S.A., Abu-Elyazeed, M.F., Elsayed, H.M. (2013) Classical methods and model predictive control of three-phase inverter with output LC filter for UPS applications. Paper presented at the 2013 International Conference on Control, Decision and Information Technologies (CoDIT).

Qin, L., Fang, Z.Z., Baoming, G. (2012) Pulse-Width-Amplitude-Modulated voltage-fed quasi-Z-source direct matrix converter with maximum constant boost. Paper presented at the Twenty-Seventh Annual IEEE Applied Power Electronics Conference and Exposition (APEC).

Rodriguez, J., Cortes, P. (2012) Predictive Control of Power Converters and Electrical Drives. John Wiley. United Kingdom.

Sharida, A., Bayhan, S., Abu-Rub, H., Fesli, U. (2024) Inverse Model Predictive Control for PowerElectronic Converters. IEEE Access, 12, 68485 – 68496. https://doi.org/10.1109/ACCESS.2024. 3395925.

Wang, L., Chai, S., Yoo, D., Gan, L., Ng, K. (2015) PID and Predictive Control of Electrical Drives and Power Converters using MATLAB / Simulink. John Wiley. Singapore.

Wensheng, S., Zhixian, D., Shunliang, W., Xiaoyun, F. (2016) A Simple Model Predictive Power Control Strategy for Single-Phase PWM Converters With Modulation Function Optimization. IEEE Transactions on Power Electronics, 31(07), 5279–5289. doi: https://doi.org/10.1109/TPEL.2015. 2481323.

Xiaowei, Y., Haitao, H., Hai, H., Yunjiang, L., Zhengyou, H. (2021) A Quasi-Resonant Extended State Observer-Based Predictive Current Control Strategy for Three-Phase PWM Rectifier. IEEE Ind Electron Mag, 69(12), 13910–13917. doi: https://doi.org/ 10.1109/TIE.2021.3137441.